

# COMPUTATIONAL MODELLING OF AUXETICS

**TOMASZ STREK**

Institute of Applied Mechanics  
Poznan University of Technology  
ul. Jana Pawla II 24, 60-965 Poznan, Poland

Date: 2018.10.11

## NEGATIVE POISSON'S RATIO

Materials with negative Poisson's ratio (NPR), at present, often referred to as auxetics [Evans, 1991], have been known for years. The key to this auxetic behavior is the negative Poisson's ratio [Love, 1892]. It is well known that the range of the Poisson's ratio for the 3D isotropic material is from -1 to 0.5, while for 2D structures this range is from -1 to 1.

In the early 1900s, a German physicist Woldemar Voigt [1928] was the first who reported this property and his work suggested that the crystals somehow become thicker laterally when stretched longitudinally nevertheless it was ignored for decades.

Typically, Poisson's ratio of isotropic materials is positive, what means that common materials shrink transversely when stretched. An auxetic material behaves differently, i.e. if it is stretched in one direction, it expands along (at least one of) the transverse directions.

Poisson's ratio is within the range  $-1 \leq \nu \leq +1/(d-1)$ . 3D isotropic systems can exhibit Poisson's ratios within the range  $-1 \leq \nu \leq +0.5$ . For anisotropic materials Poisson's ratio can have **any positive or negative values** in certain directions.

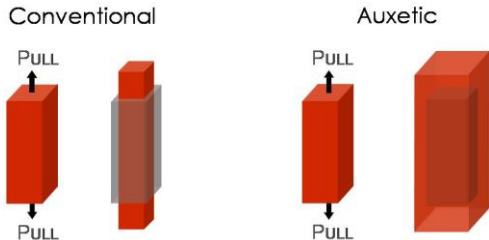
## EFFECTIVE POISSON RATIO

Effective Poisson's ratio as the negative ratio of the an average transverse to average longitudinal strain

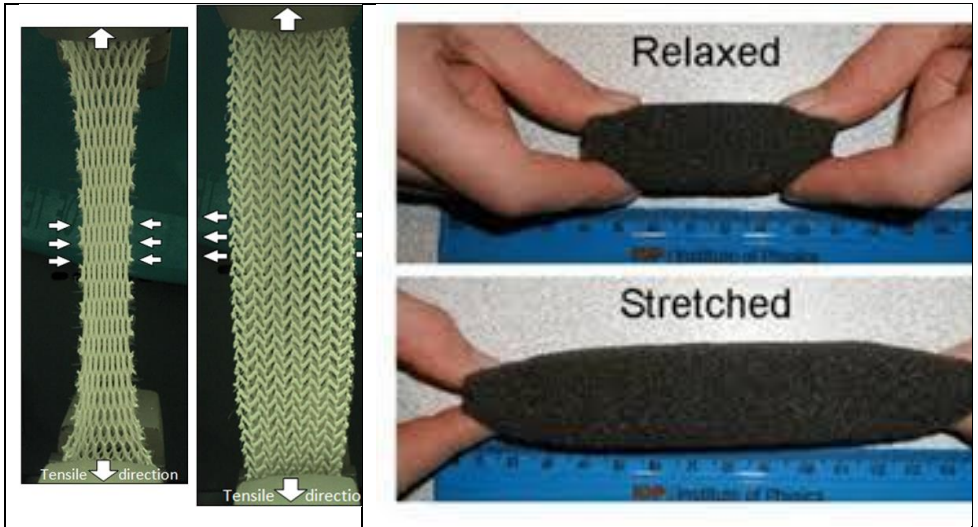
$$\nu_{eff} = -\frac{\bar{\epsilon}_{transverse}}{\bar{\epsilon}_{longitudinal}}.$$

Effective Young's modulus as the ratio of an average longitudinal stress to average longitudinal strain

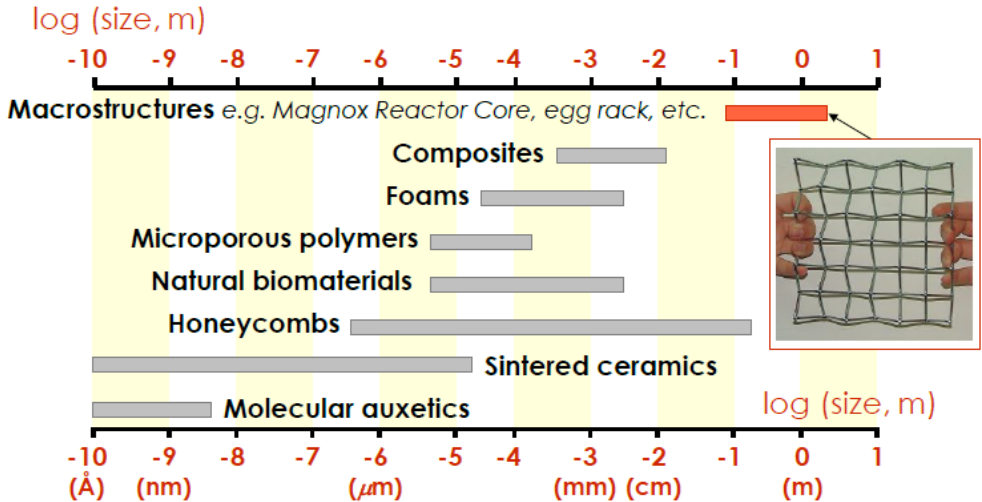
$$E_{eff} = \frac{\bar{\sigma}_{longitudinal}}{\bar{\epsilon}_{longitudinal}}.$$



## AUXETICS

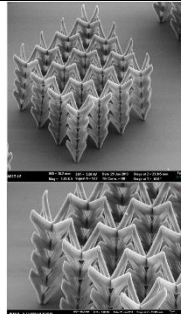
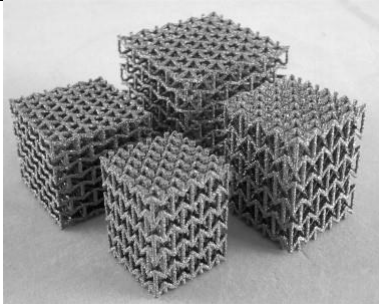
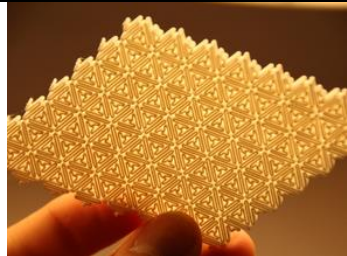
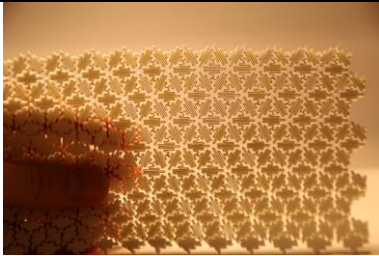


## LENGTH SCALE OF AUXETICS



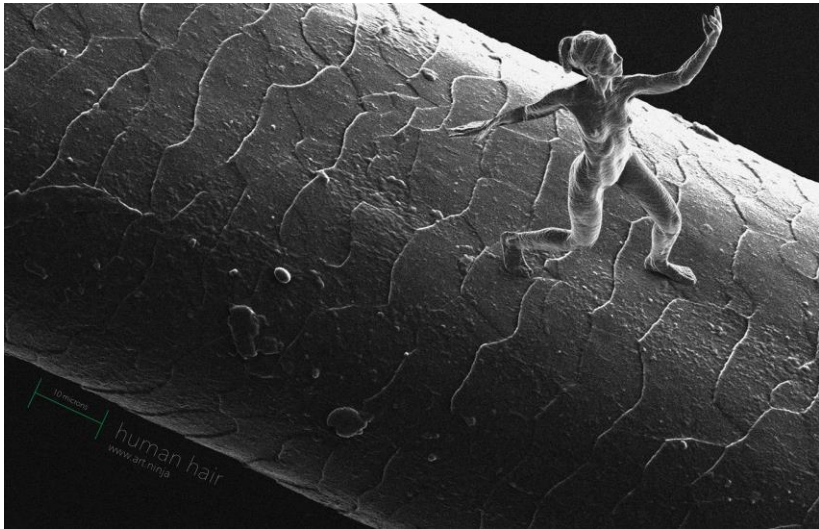
Source: Joseph N. Grima, *Auxetic Metamaterials*, 2010, [www.auxetic.info](http://www.auxetic.info)

## 3D PRINTING – MANUFACTURING

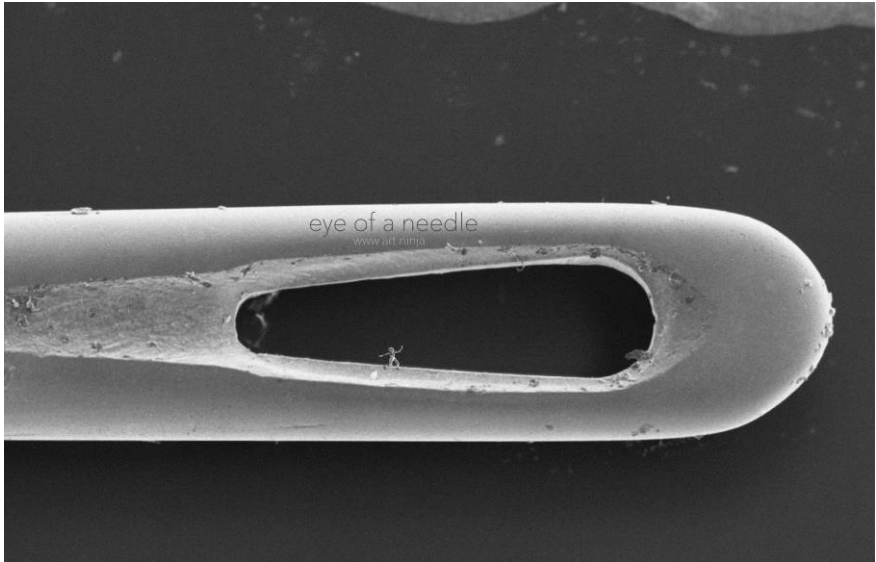


Stefan Hengsbach,  
and Andrés Díaz  
Lantada,  
Direct laser writing of  
auxetic structures:  
Present capabilities  
and challenges,  
*Smart Mater. Struct.*  
**23** 085033 2014

# NANOSCULPTURE

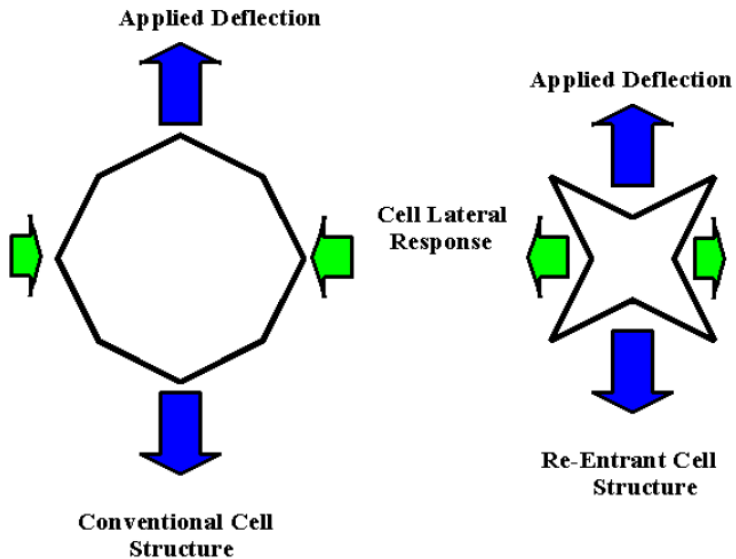


Source: <https://www.jontyhurwitz.com/portfolio/nano/>



*Source: <https://www.jontyhurwitz.com/portfolio/nano/>*

## HONEYCOMB MICROSTRUCTURE

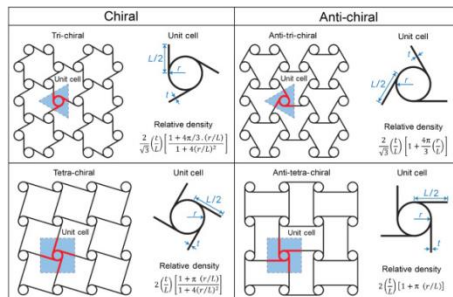


## AUXETICS STRUCTURES

**Auxetic property occurs due to their particular internal structure and the way this deforms when the sample is uniaxially loaded.**

**Auxetics** can be:

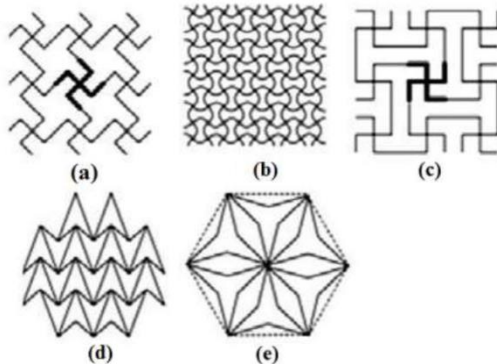
- single molecules,
- crystals, or
- a particular **structure** of macroscopic matter:
  - re-entrant structures,
  - chiral structures,
  - rotating rigid/semi-rigid units,
  - angle-ply laminates,
  - hard molecules,
  - micro porous polymers, and liquid crystalline polymer etc.



Davood Mousanezhad, Babak Haghpanah, Ranajay Ghosh, Abdel Magid Hamouda, Hamid Nayeb-Hashemi, Ashkan Vaziri,  
**Elastic properties of chiral, anti-chiral, and hierarchical honeycombs: A simple energy-based approach.**  
*Theoretical and Applied Mechanics Letters* **2016**, 6, 2, 81-96.

## 2D RE-ENTRANT STRUCTURES - EXAMPLES

There are different re-entrant structures introduced.



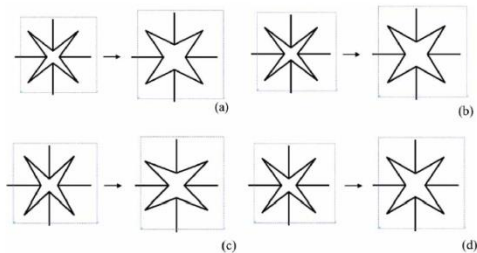
Based on their shape, they were named:

- (a) lozenge grids,
- (b) sinusoidal ligaments,
- (c) square grids,
- (d) double arrowhead, and
- (e) structurally hexagonal re-entrant honeycomb.

*Liu Y and Hu H, A review on auxetic structures and polymeric materials. Scientific Research and Essays, 2010, Vol. 5 (10), pp.1052-1063.*

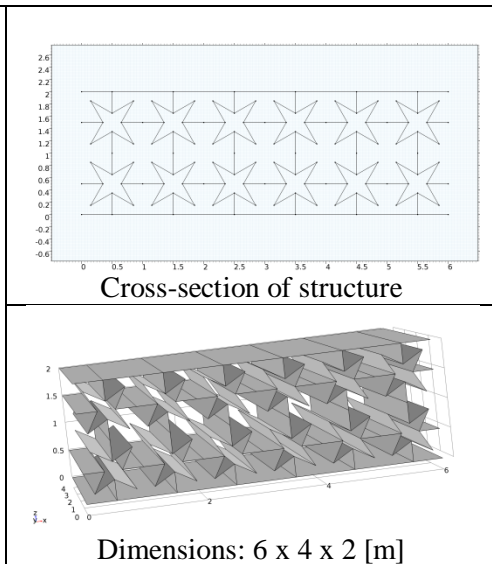
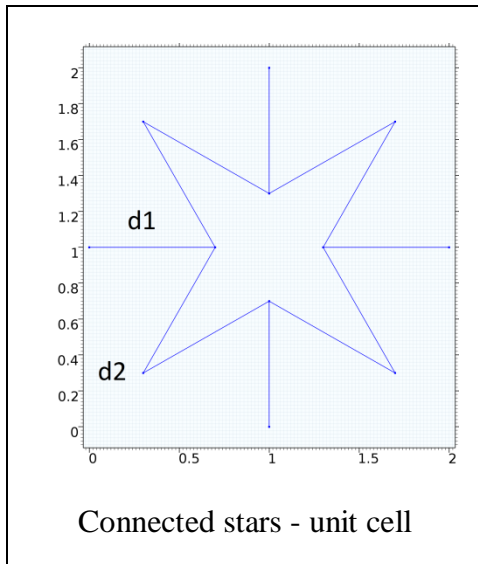
## AUXETIC MATERIALS - STAR SHAPED UNITS

In 2005 Grima and co-authors presented a class of two-dimensional periodic structures build of **star-shaped units** which are connected together to form two-dimensional periodic structures which can be described as “**connected stars**” (STAR-4 or -6 systems).



*From: J N. Grima, R. Gatt, A. Alderson and K.E. Evans, On the potential of connected stars as auxetic systems, Molecular Simulation, 31, 13, 2005, 925–935.*

# PARAMETERS OF UNIT CELL - GEOMETRY OF CORE

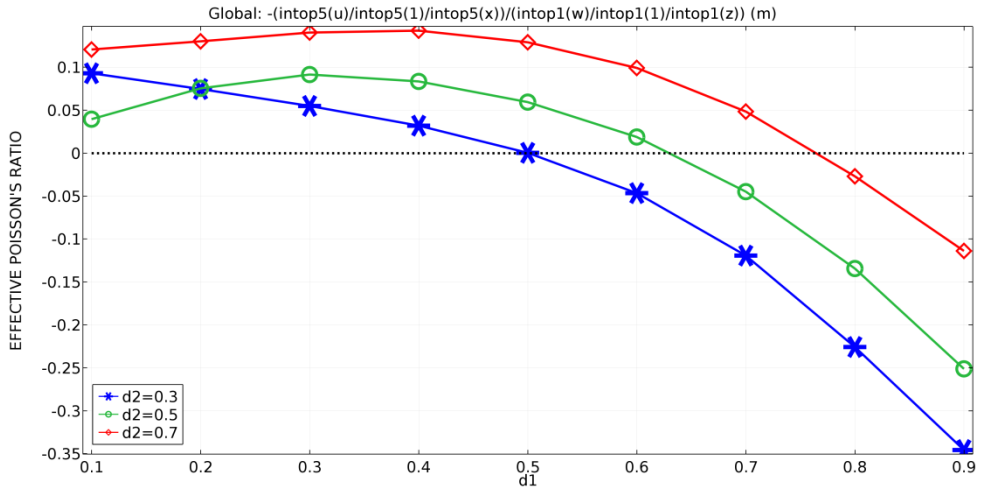


# BASIC GEOMETRIES - UNIT CELLS OF CORE

(AUXETICITY  $\rightarrow d1 > d2$ )

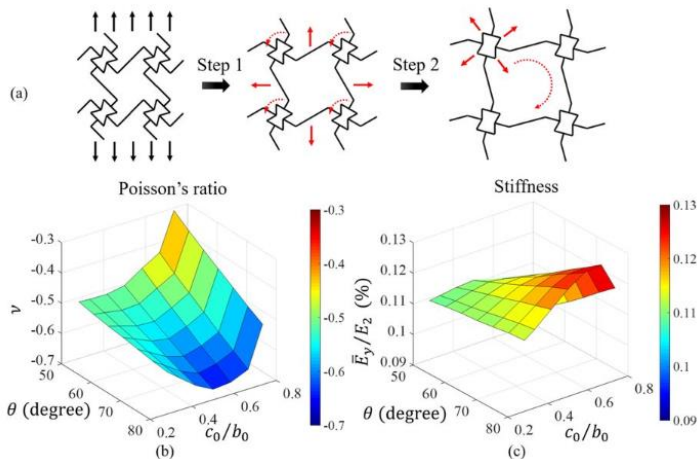
	<b>d2=0.3</b>	<b>d2=0.5</b>	<b>d2=0.7</b>
<b>d1=0.3</b>			
<b>d1=0.5</b>			
<b>d1=0.7</b>			

# EFFECTIVE POISSON'S RATIO COMPRESSION TEST



# MECHANICAL METAMATERIALS

## 3D Printed Auxetic Mechanical Metamaterial with Chiral Cells and Re-entrant Cores



Yunyao Jiang and Yaning Li, 2018

**3D Printed Auxetic Mechanical Metamaterial with Chiral Cells and Re-entrant Cores,**  
*Scientific Reports* 2018, 8, 2397. DOI: 10.1038/s41598-018-20795-2

## TWO-PHASE AUXETIC COMPOSITE BUILT OF POSITIVE PR CONSTITUENTS

- It is a common approach that auxeticity results from the geometry of the material structure so that it has some empty spaces (voids) within its structure
- Recent works shows, however, that it is possible to obtain a composite material that exhibit auxetic , although it has no voids in its volume and all its constituent material are characterized by PPR.
- Such possibility has been presented by Evans\* and in several examples within recent months\*\*.

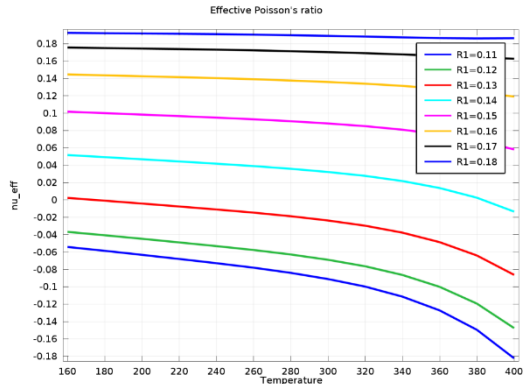
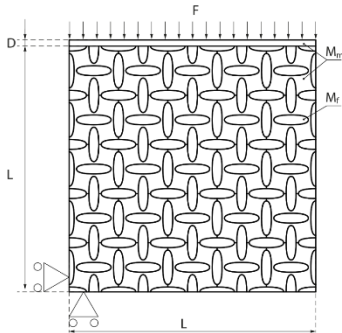
\* *K. E. Evans, M. A. Nkansah, and I. J. Hutchinson, Acta Metall. Mater. 40(9), 2463–2469*

\*\**Strek, Jopek, Nienartowicz - Dynamic response of sandwich panels with auxetic cores, PSS(B), 252, 7, pp 1540–1550, 2015 DOI: 10.1002/pssb.201552024*

\*\**Jopek, Strek, Thermal and structural dependence of auxetic properties of composite materials PSS(B), 252, 7, 1551–1558 (2015) / DOI 10.1002/pssb.201552192*

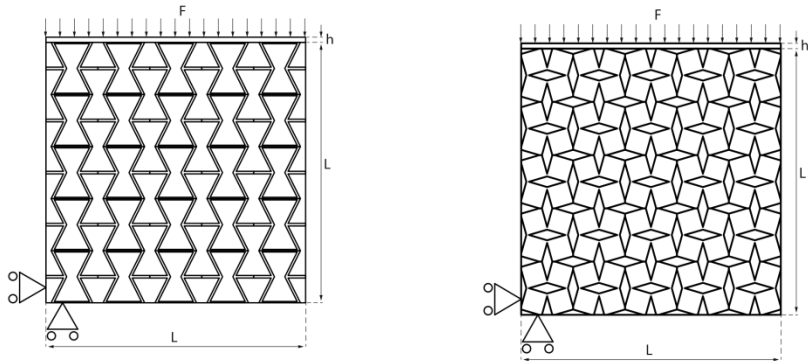
\*\* *Jopek, Strek, Thermal and structural dependence of auxetic properties of composite materials, International Conference Auxetics and other materials and models with "negative" characteristics, Poznań, 15-19 September 2014 : abstract book / ed. K. W. Wojciechowski,*

## TWO-PHASE AUXETIC COMPOSITE – EXAMPLE 1 (THERMOAUXETICITY)



Fibrous composite made of PPR materials: “hard” matrix, “soft” fibres\*  
**Thermoauxeticity** – interaction between temperature and auxeticity  
 \**Jopek, Strek, PSS(B)*, 252, 7, 1551–1558 (2015) / DOI 10.1002/pssb.201552192

## TWO-PHASE AUXETIC COMPOSITE – EXAMPLES 2-3

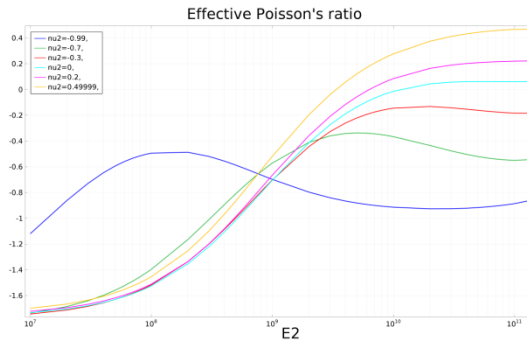
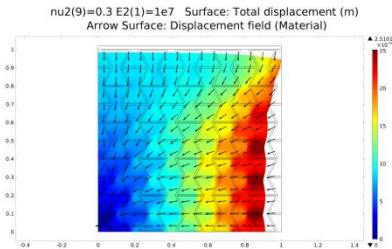


The quarter of sandwich panel

Left: (SPRH) made of cellular re-entrant honeycombs and filler material.

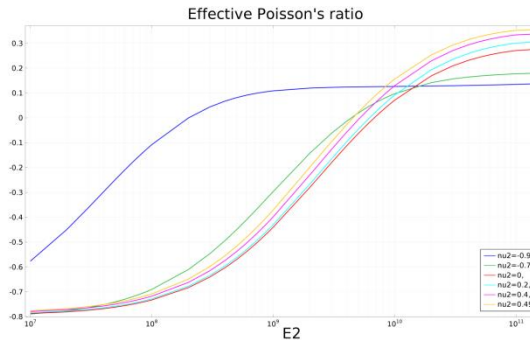
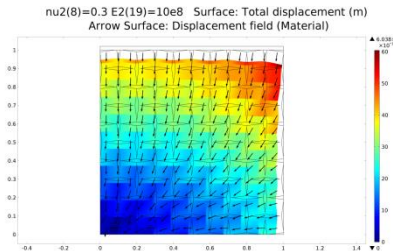
Right: (SPRS) made of cellular rotating squares and filler material

## TWO-PHASE AUXETIC COMPOSITE - EXAMPLE 2



*Strek, Jopek, Nienartowicz - Dynamic response of sandwich panels with auxetic cores, PSS(B), 252, 7, pp 1540–1550, 2015 DOI: 10.1002/pssb.201552024*

## TWO-PHASE AUXETIC COMPOSITE - EXAMPLE 3



*Strek, Jopek, Nienartowicz - Dynamic response of sandwich panels with auxetic cores, PSS(B), 252, 7, pp. 1540–1550, 2015 DOI: 10.1002/pssb.201552024*

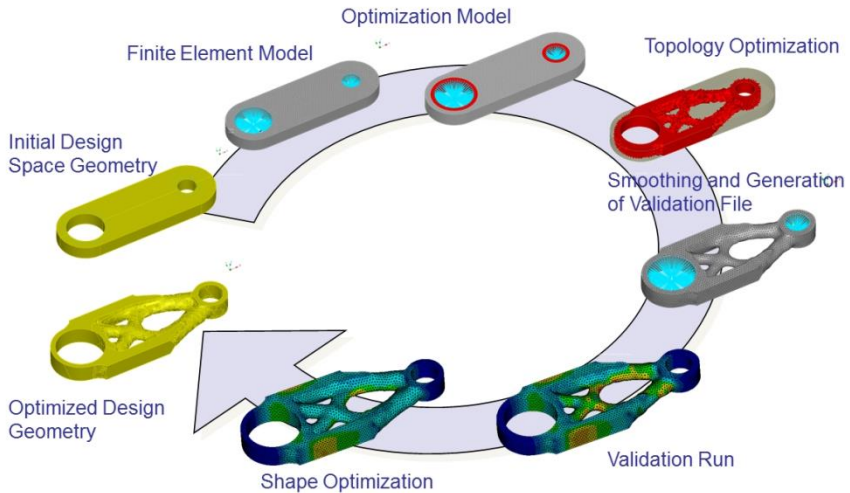
## **COMPOSITE MATERIAL DESIGN USING TOPOLOGY OPTIMIZATION METHOD**

**A composite is a mixture of two or more distinct constituents or phases.** The purpose of composite material design is to generate materials with improved or prescribed property that can't be found in usual material.

The inclusions such as fiber, sphere-reinforced and laminated materials are commonly used to achieve this purpose. In this type of approach, the location, orientation and volume fraction of the fiber, particulate or lamina are considered during the design process.

**The topology optimization method is a promising new technique for the systematic design of composite material.** A richer and wider class of material properties can be achieved by using the topology optimization method.

# TOPOLOGY OPTIMIZATION



From: <http://wildeanalysis.co.uk/fea/software/tosca>

## MATERIALS WITH EXTREME THERMAL EXPANSION

**Sigmund and Torquato [1997] generated composite materials with extreme thermal expansion coefficients using a three-phase topology optimization method.**

The three-phase are: two different material phases and a void phase. The effective thermoelastic properties of the material are considered as the objective function, subject to constraints on elastic symmetry and volume fractions of the constituent phase.



Figure: Optimal microstructures for minimization of effective thermal strain coefficient [Sigmund and Torquato, 1997]

## MATERIALS WITH EXTREME ELASTICITY PROPERTIES

Yi et al. [2000] used the topology optimization method to find an optimal distribution of two viscoelastic phases, so that the stiffness and damping characteristic of the composite material will be optimum. The design constraints are volume fraction, effective complex moduli, geometric symmetry and material symmetry.

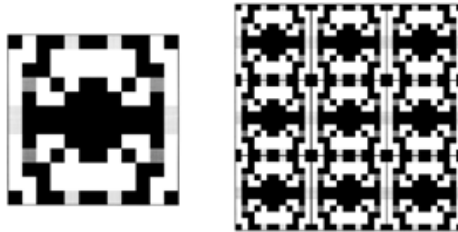


Figure: The microstructure of viscoelastic composite material example [Yi et al., 2000]. The gray elements represent intermediate phase.

## NPR GENERATED BY TOPOLOGY OPTIMIZATION

Larsen et al. [1997] generated a material with negative Poisson's ratio using topology optimization. Figure shows the microstructure of the composite material with a negative Poisson's ratio of  $-0.8$ .

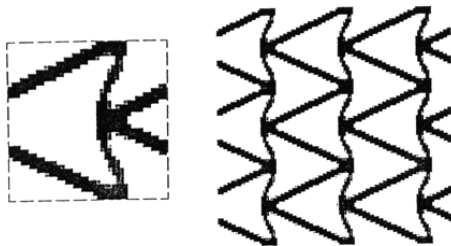


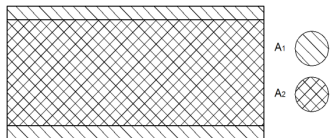
Figure: The microstructure of negative Poisson's ratio composite material [Larsen et al., 1997]

## MATERIAL PARAMETERS

Isotropic materials parameters used in optimization are:

- for the **soft material**: density is  $\rho_1=4000 \text{ kg/m}^3$ , Young modulus is  $E_1=1\text{e}+7 \text{ Pa}$ , and the Poisson's ratio is  $\nu_1=0.1$ ;
- for the **hard material (structural steel)**: density is  $\rho_2=7850\text{kg/m}^3$ , Young modulus is  $E_2=2\text{e}+11 \text{ Pa}$  and the Poisson's ratio is  $\nu_2=0.33$ .

Outer layers consist of the hard material, while the middle layer is a two-phase material composite. Only the middle layer is subjected to minimization by the objective function defined as the minimum of Poisson's ratio value.



Middle composite layer consists of  $frac = 20\% \text{ or } 40\%$  (fraction) of hard material:  $V_f = A_f \cdot A_2$  and  $A_f = frac / 100\%$

## **SOLID ISOTROPIC MATERIAL WITH PENALIZATION (SIMP) MODEL**

Using SIMP model generalized material parameters (e.g. Young's modulus, Poisson ratio or density) can be approximated as a function of control variable.

Using SIMP model one can write the generalized Young's modulus for two-phase composite material as

$$E(r) = E_1 + (E_2 - E_1)r(\mathbf{x})^p, \quad (1.1)$$

where  $E_1$  and  $E_2$  are the Young's modulus of first and second material and  $E_1 < E_2$ ,  $p > 1$  is a penalty parameter.

In the same manner the generalized Poisson's ratio for  $\nu_1 < \nu_2$  is

$$\nu(r) = \nu_1 + (\nu_2 - \nu_1)r(\mathbf{x})^p. \quad (1.2)$$

## DESIGN CONTROL VARIABLE

The control variable,  $r(\mathbf{x})$ , which can be interpreted as a generalized material density, is required to satisfy the following constraints:

$$\begin{aligned} 0 \leq \int_V r(\mathbf{x}) dV \leq V_f \\ 0 \leq r(\mathbf{x}) \leq 1 \end{aligned} \tag{1.3}$$

where  $V_f$  is the **material volume** available for distribution (**volume fraction**).

## EFFECTIVE POISSON RATIO

One can define effective Poisson's ratio as the negative ratio of the an average transverse to average longitudinal strain

$$\nu_{eff} = -\frac{\bar{\varepsilon}_{transverse}}{\bar{\varepsilon}_{longitudinal}}, \quad (2.1)$$

and effective Young's modulus as the ratio of an average longitudinal stress to average longitudinal strain

$$E_{eff} = \frac{\bar{\sigma}_{longitudinal}}{\bar{\varepsilon}_{longitudinal}}. \quad (2.2)$$

The average stress and the average strain are defined as

$$\bar{\sigma} = \frac{1}{S} \int_S \sigma dS, \quad \bar{\varepsilon} = \frac{1}{S} \int_S \varepsilon dS \quad (2.3)$$

where  $\sigma$  and  $\varepsilon$  are in given direction (longitudinal or transverse) and  $S$  is the volume of the considered composite.

## EFFECTIVE POISSON RATIO

In the considered cases, the **effective Poisson's ratio** were rewritten as **dependant of the control variable**  $r = r(x)$  :

$$\nu_{eff}(r) = -\frac{\bar{\varepsilon}_{transverse}(r)}{\bar{\varepsilon}_{longitudinal}(r)}. \quad (2.4)$$

## APPLIED CONSTRAINS

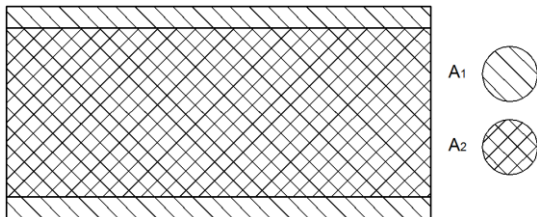
Applied constrains: pointwise inequality, which fulfills the formula:

$$0 < r(x) < 1 \text{ for } x \in A_2 \quad (2.5)$$

The second is the integral inequality:

$$0 < \int_{A_2} r(x) dA < A_f A_2 \quad (2.6)$$

where  $A_f$  is A fraction of the domain to use for the distribution of the second material,  $A_1$  and  $A_2$  are areas of the considered domain.



## MECHANICAL GOVERNING EQUATIONS

The elastic isotropic state is governed by the following equations, laws and rules.

When we neglect the body force the Navier's equation in steady state

$$-\nabla \cdot \boldsymbol{\sigma} = \mathbf{0} \quad (3.1)$$

where  $\boldsymbol{\sigma}$  is the stress tensor.

The constitutive law (the stress-strain relation) for linear conditions reads:

$$\boldsymbol{\sigma} = \mathbf{D} \boldsymbol{\varepsilon}, \quad (3.2)$$

where  $\boldsymbol{\sigma}$  is the stress tensor,  $\boldsymbol{\varepsilon}$  is the small strain tensor  $\boldsymbol{\varepsilon} = \frac{1}{2}(\nabla \mathbf{u} + (\nabla \mathbf{u})^T)$

(superscript  $T$  denotes transpose of matrix or vector) and  $\mathbf{D}$  is the elastic matrix -  $\mathbf{S} = \mathbf{D}^{-1}$  is compliance matrix.

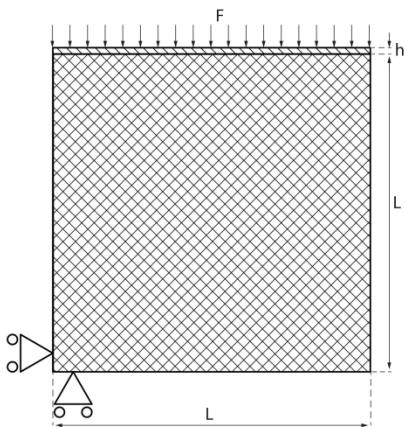
**The stress and strain components** are described in **vector form** with the six stress and strain components in column vectors:

$$\begin{aligned}\boldsymbol{\sigma} &= \begin{bmatrix} \sigma_x & \sigma_y & \sigma_z & \tau_{xy} & \tau_{yz} & \tau_{xz} \end{bmatrix}^T, \\ \boldsymbol{\varepsilon} &= \begin{bmatrix} \varepsilon_x & \varepsilon_y & \varepsilon_z & \gamma_{xy} & \gamma_{yz} & \gamma_{xz} \end{bmatrix}^T.\end{aligned}\tag{3.3}$$

Linear Hooke law - isotropic material of components Lamé's constants  $\lambda$  and  $\mu$  in terms of Young's modulus,  $E$ , and Poisson's ratio,  $\nu$ , are the following:

$$\lambda = \frac{E\nu}{(1+\nu)(1-2\nu)}, \quad \mu = \frac{E}{2(1+\nu)}.\tag{3.4}$$

## BOUNDARY CONDITIONS (quarter of structure)



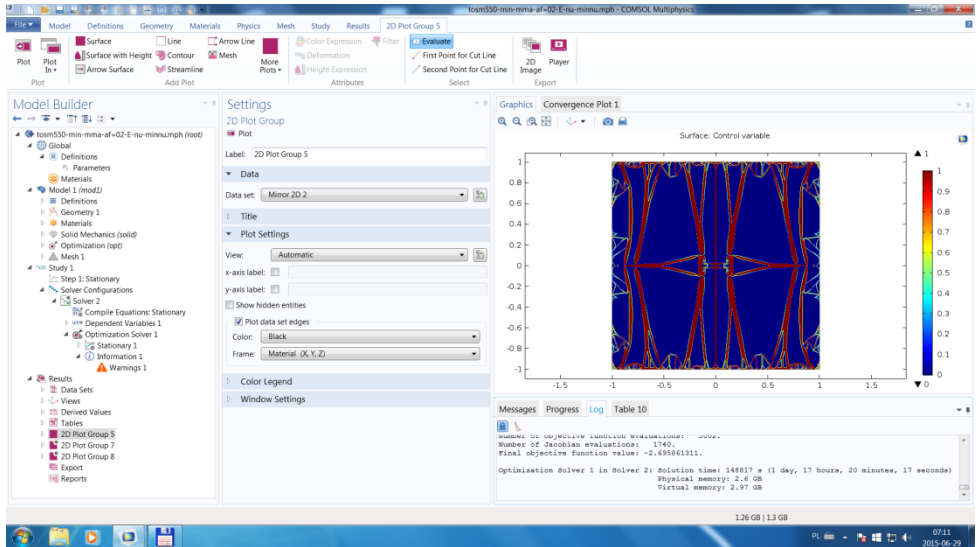
**RIGHT:**  $x=L$  and  $y \in \langle 0, L+h \rangle$  - free BC;

**LEFT (SYMMETRY):**  $x=0$  and  $y \in \langle 0, L+h \rangle$  - roller BC:  $\mathbf{n} \cdot \mathbf{u} = 0$ ;

**BOTTOM (SYMMETRY):**  $y=0$  and  $x \in \langle 0, L \rangle$  - roller BC:  $\mathbf{n} \cdot \mathbf{u} = 0$ ;

**TOP:**  $y=L+h$  and  $x \in \langle 0, L \rangle$  - boundary load:  $\boldsymbol{\sigma} \cdot \mathbf{n} = \mathbf{F}$ , where  $\mathbf{F} = (0, -F_L)$ , where  $\mathbf{n}$  is the normal unit vector to boundary

# COMSOL MULTIPHYSICS MODELING SOFTWARE



## NUMERICAL RESULTS – TWO-PHASE AUXETIC

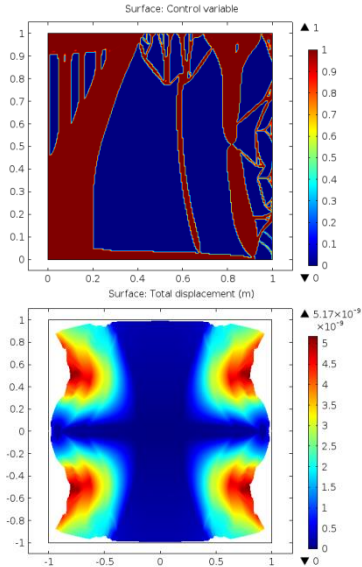


**Figure:** (TOP) Distribution of two materials in compressed composite obtained using topology optimization (quarter and full). **Blue color represents soft material and red is hard structural steel** and (BOTTOM) deformation of auxetic structure ( $A_f = 0.4$ ,  $\nu_{eff} = -3.18$ )

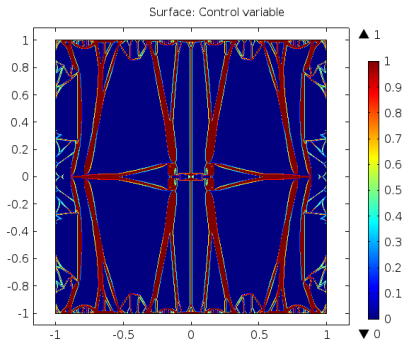


**Figure:** Distribution of two materials in compressed composite obtained using topology optimization  
 ( $A_f = 0.2$ ,  $v_{eff} = -2.69$ )

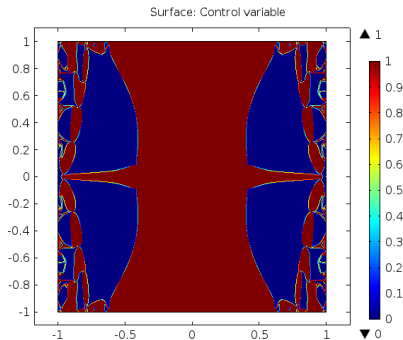
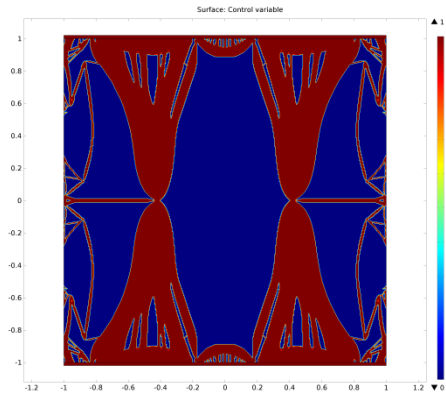
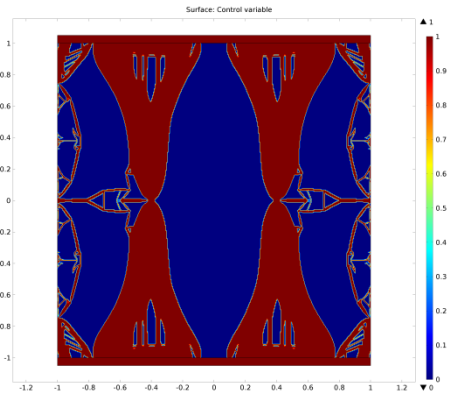


**Figure:** Distribution of two materials in compressed composite  
 ( $A_f = 0.6$ ,  $v_{eff} = -3.49$ )

## THREE-LAYERS SANDWICH STRUCTURE – $A_f=0.4$

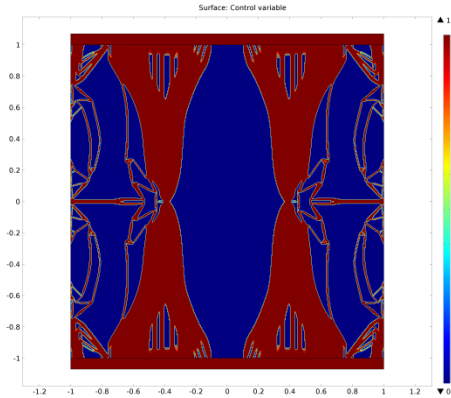


$$A_f = 0.4, \quad h = 0.02, \quad L = 1, \quad v_{eff} = -3.72$$

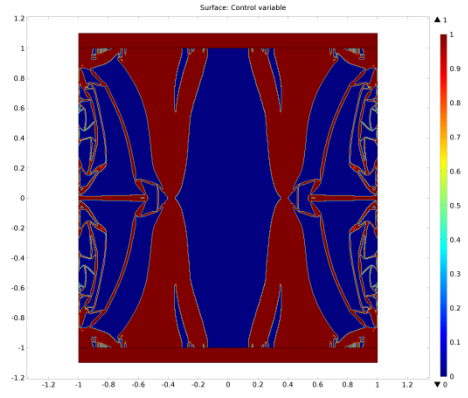


$$A_f = 0.4, \quad h = 0.05, \quad L = 1, \quad v_{eff} = -3.82$$

## THREE-LAYERS SANDWICH STRUCTURE – $A_f=0.4$

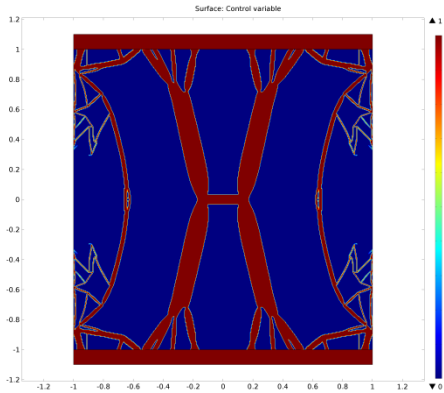


$$A_f = 0.4, \quad h = 0.07, \quad L = 1, \quad v_{eff} = -3.73$$

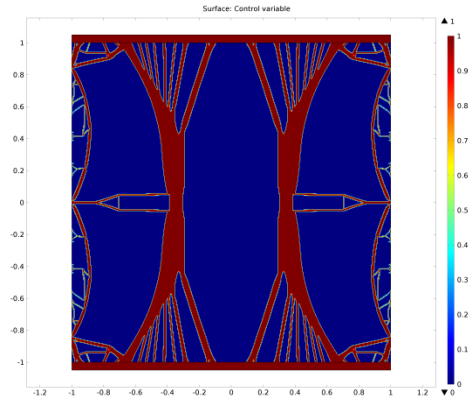


$$A_f = 0.4, \quad h = 0.1, \quad L = 1, \quad v_{eff} = -3.83$$

## THREE-LAYERS SANDWICH STRUCTURE – $A_f=0.2$

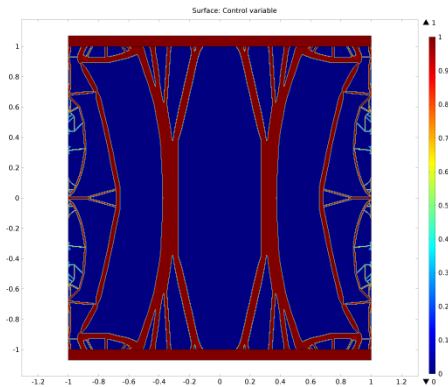


$$A_f = 0.2, \quad h = 0.02, \quad L = 1, \quad v_{eff} = -2.75$$

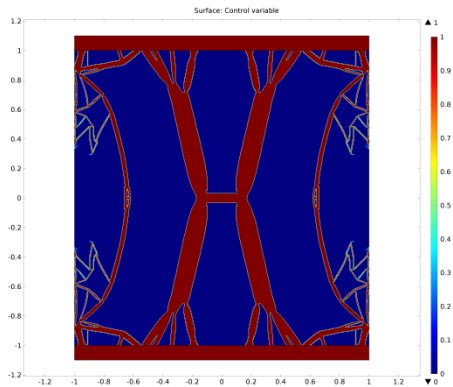


$$A_f = 0.2, \quad h = 0.05, \quad L = 1, \quad v_{eff} = -3.17$$

## THREE-LAYERS SANDWICH STRUCTURE – $A_f=0.2$



$$A_f = 0.2, \quad h = 0.07, \quad L = 1, \quad v_{eff} = -3.48$$



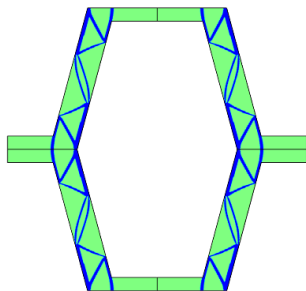
$$A_f = 0.2, \quad h = 0.1, \quad L = 1, \quad v_{eff} = -2.75$$

# STRUCTURES WITH NON-INTUITIVE BEHAVIOUR

## HONEYCOMB TOPOLOGY OPTIMIZATION

A

Optimized distribution of  
constituents



RE =

$10^2$

$A_f =$

0.2

1

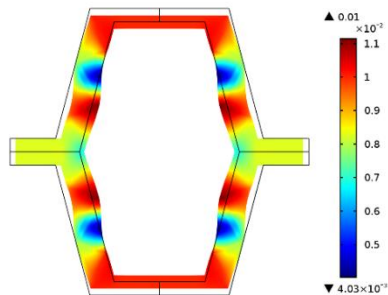
$t = 0.2$

$v_{eff} =$

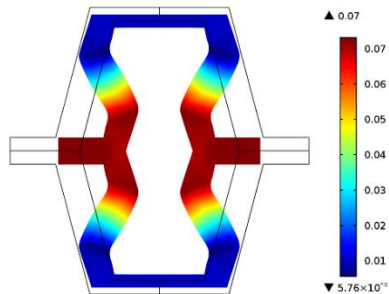
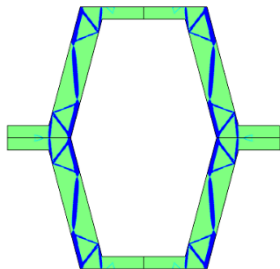
0.78

B

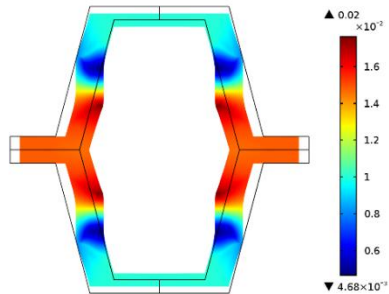
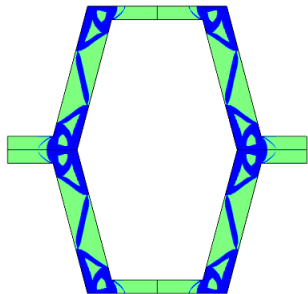
Deformed shaped and  
displacement field



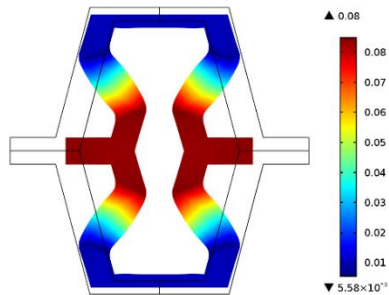
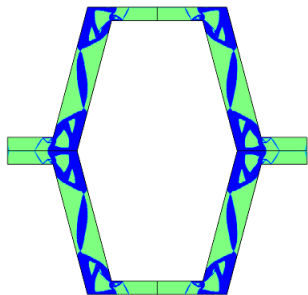
2  
RE =  
 $10^3$   
 $A_f =$   
0.2  
 $t = 0.2$   
 $V_{eff} =$   
6.91



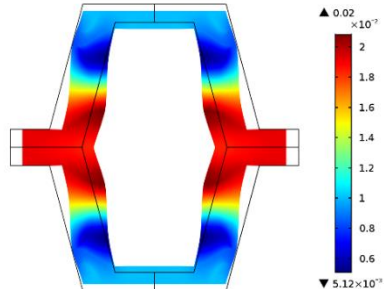
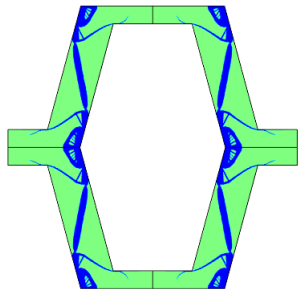
3  
RE =  
 $10^2$   
 $A_f =$   
0.4  
 $t = 0.2$   
 $V_{eff} =$   
1.41



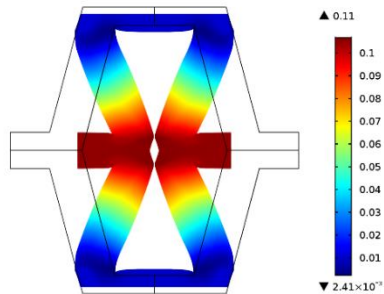
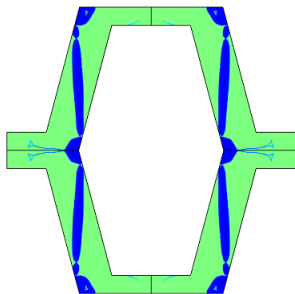
4  
RE =  
 $10^3$   
 $A_f =$   
0.4  
 $t = 0.2$   
 $V_{eff} =$   
7.95



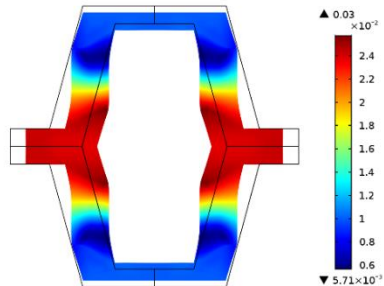
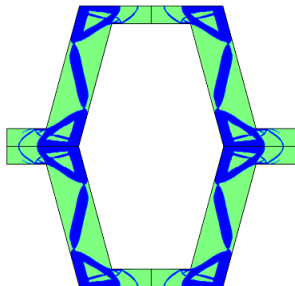
5  
RE =  
 $10^2$   
 $A_f =$   
0.2  
 $t = 0.2$   
8  
 $V_{eff} =$   
1.89



6  
 $RE = 10^3$   
 $A_f = 0.2$   
 $t = 0.2$   
 $V_{eff} = 10.33$

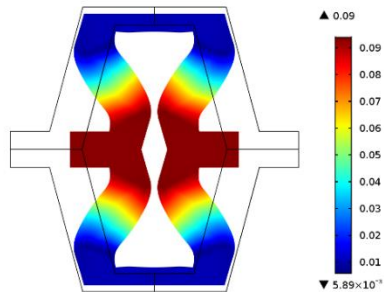
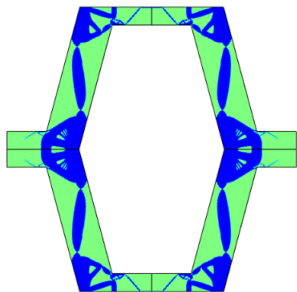


7  
 $RE = 10^2$   
 $A_f = 0.4$   
 $t = 0.2$   
 $V_{eff} = 2.39$



8

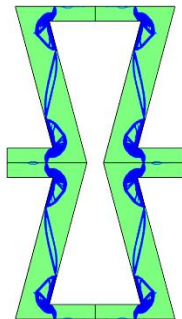
RE =  
 $10^3$   
 $A_f =$   
0.4  
 $t = 0.2$   
8  
 $v_{\text{eff}} =$   
9.17



## RE-ENTRANT HONEYCOMB TOPOLOGY OPTIMIZATION

A

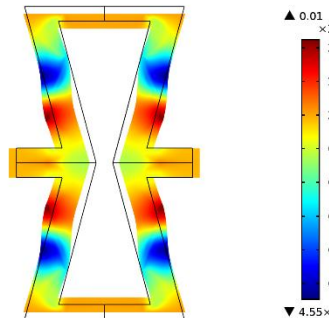
Optimized distribution of  
constituents



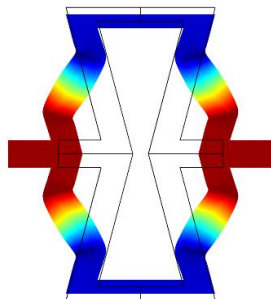
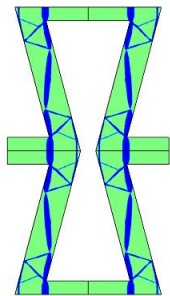
1 RE =  
10<sup>2</sup>  
A<sub>f</sub> =  
0.2  
t = 0.2  
V<sub>eff</sub>  
= 1.74

B

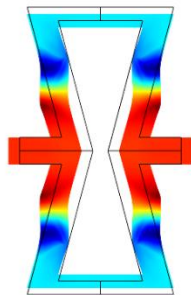
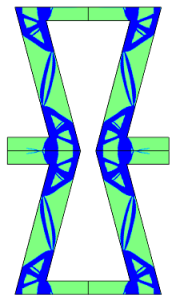
Deformed shaped and  
displacement field



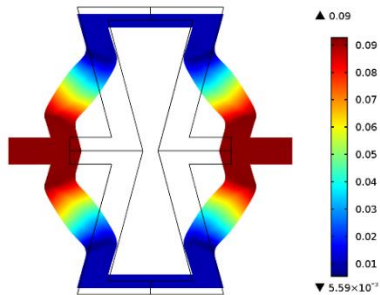
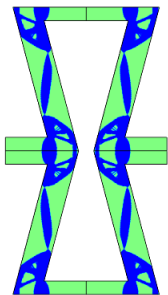
2  
 $RE = 10^3$   
 $A_f = 0.2$   
 $t = 0.2$   
 $V_{eff} = 12.9$   
 7



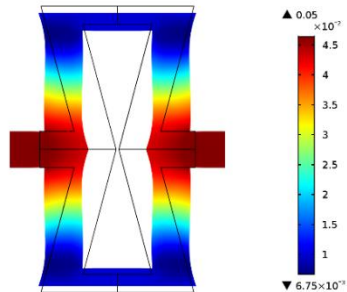
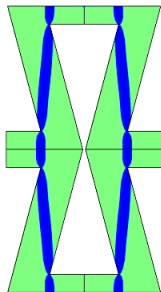
3  
 $RE = 10^2$   
 $A_f = 0.4$   
 $t = 0.2$   
 $V_{eff} = 2.95$



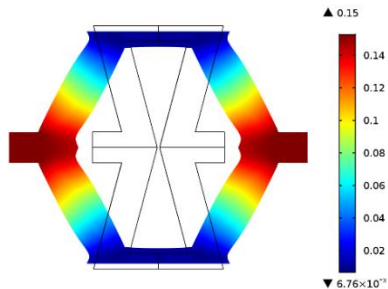
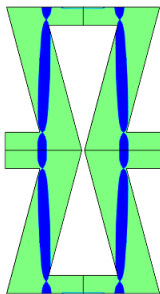
4  
 $RE = 10^3$   
 $A_f = 0.4$   
 $t = 0.2$   
 $V_{eff} = 16.1$   
 1



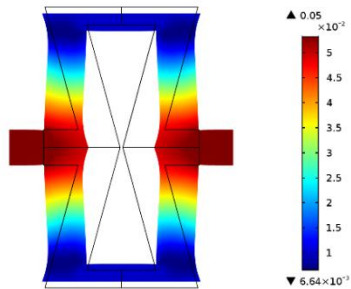
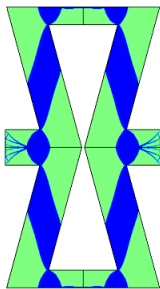
5  
 $RE = 10^2$   
 $A_f = 0.2$   
 $t = 0.2$   
 8  
 $V_{eff} = 8.42$



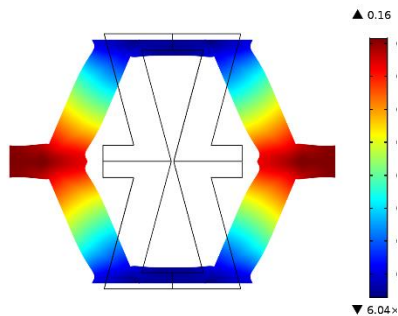
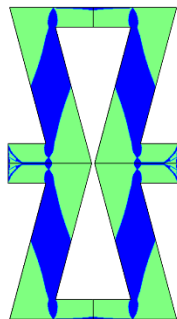
6  
 RE =  
 $10^3$   
 $A_f =$   
 0.2  
 $t = 0.2$   
 8  
 $v_{eff}$   
 $= 27.8$   
 4



7  
 RE =  
 $10^2$   
 $A_f =$   
 0.4  
 $t = 0.2$   
 8  
 $v_{eff}$   
 $= 9.67$



8  
RE =  
 $10^3$   
 $A_f =$   
0.4  
 $t = 0.2$   
8  
 $V_{eff}$   
 $= 29.7$



Strek, T.; Jopek, H.; Idczak, E.; Wojciechowski, K.W.  
Computational Modelling of Structures with Non-Intuitive Behaviour.  
*Materials* **2017**, *10*, 1386.

## SUMMARY AND CONCLUSIONS

- In the present paper we have shown explicitly FEM applicability to study auxetic material or sandwich panel with auxetic phase.
- Geometric structure of core and its parameters have great influence on mechanical properties of auxetic material.
- Auxetic characteristic of sandwich panel core were obtained using topology optimization. Two-phase composite with negative Poisson's ratio was generated using topology optimization.
- In general, all gained topology structures have complicated shapes. Irregular shapes structures can achieve smaller values of Poisson's ratio.
- Auxeticity of composite materials depends not only on topology of its constituents, but also on the ratio of its Young's moduli and PR.

# THANK YOU FOR YOUR ATTENTION

## ***ACKNOWLEDGMENTS***

*This work has been supported by a grant from the Ministry of Science and Higher Education in Poland: 02/21/DSPB/3513/2018. The simulations have been made at the Institute of Applied Mechanics, Poznan University of Technology.*

## **FREQUENCY RESPONSE FUNCTIONS (FRF)**

**Engineering dynamics** is strongly based on the modelling, analysis, and prediction of vibration of a physical system. **Vibration** could result from harmonic load acting on system or motion with damping. It could be described with the use of multiple parameters. One of them is **frequency response function (FRF)** which is widely used in many fields of engineering and plays an important role in many applications of linear vibrations analysis.

**Different types of frequency response functions** [Gatti, 2014] are known in engineering issues e.g.:

- displacement to force ratio which is called receptance,
- admittance or dynamic compliance;
- velocity to force ratio called mobility;
- acceleration to force ratio which is accelerance or inertance;
- force to displacement ratio that is called dynamic stiffness;
- force to velocity ratio which is mechanical impedance and
- force to acceleration ratio called an apparent mass.

$$\text{Accelerance} = \frac{\text{Acceleration}}{\text{Force}}$$

$$\text{Apparent Mass} = \frac{\text{Force}}{\text{Acceleration}}$$

$$\text{Mobility} = \frac{\text{Velocity}}{\text{Force}}$$

$$\text{Impedance} = \frac{\text{Force}}{\text{Velocity}}$$

$$\text{Receptance} = \frac{\text{Displacement}}{\text{Force}}$$

$$\text{Dynamic Stiffness} = \frac{\text{Force}}{\text{Displacement}}$$

## MECHANICAL IMPEDANCE

Mechanical impedance is formally defined for linear systems over the domain of frequency as the ratio of the Fourier transforms of the force excitation and the velocity response. The frequency-dependent characteristic property of the system [On, 1967] can be written as:

$$\sum_{j=0}^N Z_{ij} v_j = F_i \quad (2.1)$$

or, in the matrix form,

$$[Z_{ij}]\{v_j\} = \{F_i\} \quad (2.2)$$

where  $i=1\dots N, j=1\dots N$  and  $N$  denotes the number of degrees of freedom.

The elements  $Z_{ij}$  are complex number that express the ratio of the transform vibratory force at coordinate  $i$  to the transform vibratory velocity at coordinate  $j$ . They are dependent on frequency and may be called impedance parameters of the system. In the case of  $i=j$ , the  $Z_{ij}$  are called **point impedance parameters**, and for all  $i \neq j$ , they are called **transfer impedance parameters**.

However,  $Z_{ij}$  maybe also considered as the ratio of the force input at the  $i$ -th coordinate to the velocity response at the  $j$  coordinate when all other coordinates are infinitely restrained (i.e., zero velocities).

Moreover, the matrix  $[Z_{ij}]$  could be considered as the mechanical impedance matrix of the system, while the column matrix  $\{v_j\}$  represents the transform of velocities corresponding to the transform of input forces  $\{F_i\}$ .

## POINT IMPEDANCE PARAMETER (DRIVING POINT IMPEDANCE)

When the force and velocity are measured at the same point and in the same direction, the ratio is denoted as the **point impedance parameter (or the driving point impedance)**.

If the force and velocity are measured in different directions or at different points, one defines the ratio as the **transfer impedance** [Gerdeen, 1975].

In most cases, however, the term mechanical impedance means a driving point mechanical impedance. The mechanical impedance  $\bar{Z}$  at the driving frequency  $\omega$  is defined mathematically as:

$$\bar{Z}(\omega) = \frac{\bar{F}(\omega)}{\bar{v}(\omega)} = \frac{F_0 e^{i\omega t}}{v_0 e^{i(\omega t - \varphi)}} = Z e^{i\varphi}, \quad (2.3)$$

where  $\omega$  is the angular frequency,  $\omega = 2\pi \text{ freq}$ ,  $F_0$  is the amplitude of a harmonic force,  $v_0$  is the amplitude of the velocity in direction of a force and  $\varphi$  is the phase angle by which the force leads the velocity.

## AVERAGE MECHANICAL IMPEDANCE

The mechanical impedance can be divided into its real and imaginary parts

$$\bar{Z}(\omega) = Ze^{i\varphi} = R + iS, \quad (2.4)$$

where  $R$  is the real part called the **mechanical resistance**,  $S$  is the imaginary part called the **mechanical reactance** and  $\tan \varphi = S/R$ .

To describe the dynamic characteristic of whole structure  $\Omega$  one can introduce **average mechanical impedance**. It can be defined as:

$$\langle Z \rangle = \frac{F_0}{\left( \int_{\Omega} v_0 d\Omega / \int_{\Omega} d\Omega \right)}. \quad (2.5)$$

## SPECIFIC STIFFNESS

Application of materials requires not only its high strength and high stiffness properties, but also its light weight. **For low-density materials, their strength and stiffness are not prominent, but the ratios of strength and stiffness to density are high**, such as magnesium alloys, composites, and honeycombs.

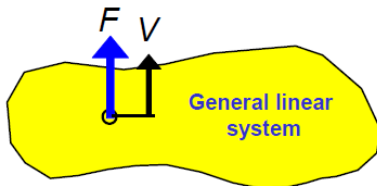
To facilitate the comparison of deformation resistance of various metamaterials, the concept of **Specific Stiffness** is introduced, which is defined as the ratio of tensile stiffness to the density of materials. The expression of the specific stiffness

$$\langle K \rangle = \frac{F_0/w_0}{m/V} = \frac{F_0 / \left( \int_{\Omega} w_0 d\Omega / \int_{\Omega} d\Omega \right)}{\left( \int_{\Omega} \rho d\Omega / L^3 \right)} \quad (2.6)$$

where  $F_0$  is the amplitude of a harmonic force in z-axis and  $w_0$  is amplitude of displacement in z-axis,  $m$  is mass of unit cell and  $V$  is volume of wrapping of unit cell.

## MOBILITY AND IMPEDANCE \*

- The response of a structure to a harmonic force can be expressed in terms of its mobility or impedance



At frequency  $\omega$  the velocity can be written in complex notation  $v(t) = Ve^{j\omega t}$

$V$  is the complex amplitude.

Similarly for the force  $f(t) = Fe^{j\omega t}$

The **mobility** is defined as

$$\text{Mobility} = \frac{V(j\omega)}{F(j\omega)}$$

The **impedance** is defined as

$$\text{Impedance} = \frac{F(j\omega)}{V(j\omega)}$$

- If the force and velocity are at the same point this is a 'point' mobility
- If they are at different points it is a 'transfer' mobility

**Note that both mobility and impedance are frequency domain quantities**

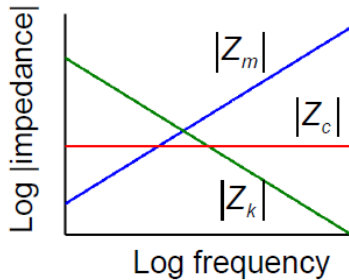
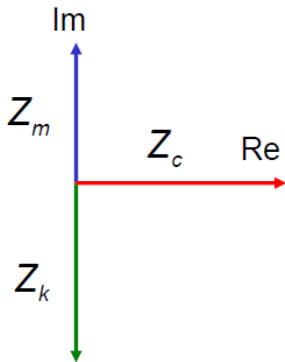
\* Mike Brennan, *Mobility and Impedance Methods*

## IMPEDANCE OF SIMPLE ELEMENTS

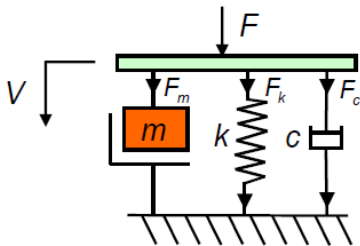
• **Spring**  $Z_k = \frac{k}{j\omega} = \frac{-jk}{\omega}$

• **Damper**  $Z_c = c$

• **Mass**  $Z_m = j\omega m$



## SIMPLE ELEMENTS IN PARALLEL



$$F = F_m + F_k + F_c$$

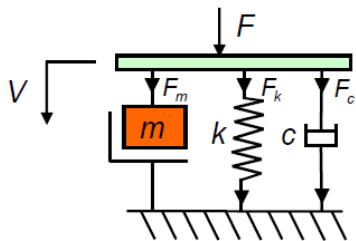
- **Point Impedance**

$$Z_{11} = j\omega m + \frac{k}{j\omega} + c$$

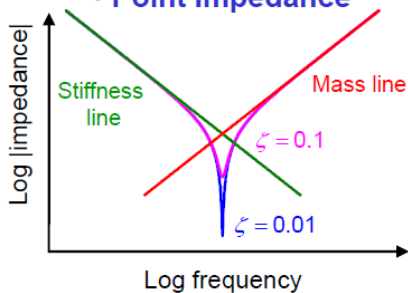
- **Point Mobility**

$$Y_{11} = \frac{1}{j\omega m + \frac{k}{j\omega} + c}$$
$$= \frac{j\omega}{k - \omega^2 m + j\omega c}$$

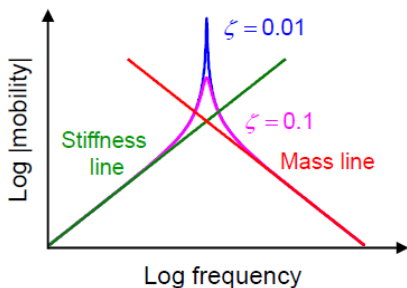
At low frequency stiffness dominates  
At resonance damping dominates  
At high frequency mass dominates



• **Point Impedance**



• **Point Mobility**



## SIMPLE ELEMENTS IN SERIES

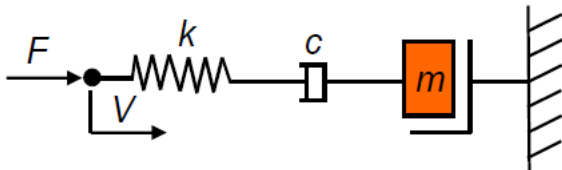
- **Impedances**

$$\frac{1}{Z_{\text{total}}} = \sum_{j=1}^N \frac{1}{Z_j}$$

- **Mobilities**

$$Y_{\text{total}} = \sum_{j=1}^N Y_j$$

- **Example**

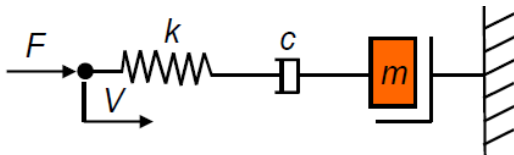


- **Point Mobility**

$$Y_{11} = \frac{j\omega}{k} + \frac{1}{c} + \frac{1}{j\omega m}$$

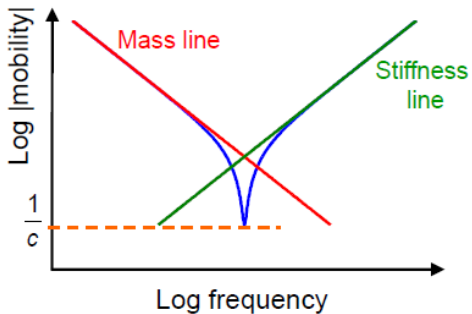
- **Point Impedance**

$$Z_{11} = \frac{1}{\frac{j\omega}{k} + \frac{1}{c} + \frac{1}{j\omega m}}$$



- **Point mobility**

At low frequency mass dominates  
 At resonance damping dominates  
 At high frequency stiffness dominates



## SOLID MECHANICS - NAVIER'S EQUATION OF MOTION

Assuming harmonic motion of the structure we can write displacement vector in the form of:

$$\mathbf{u}(x, t) = \mathbf{u}(x)e^{-i\omega t} \quad (3.1)$$

and finally the Navier's equation of motion as:

$$\rho\omega^2\mathbf{u} - \nabla \cdot \boldsymbol{\sigma} = \mathbf{F}e^{i\varphi}. \quad (3.2)$$

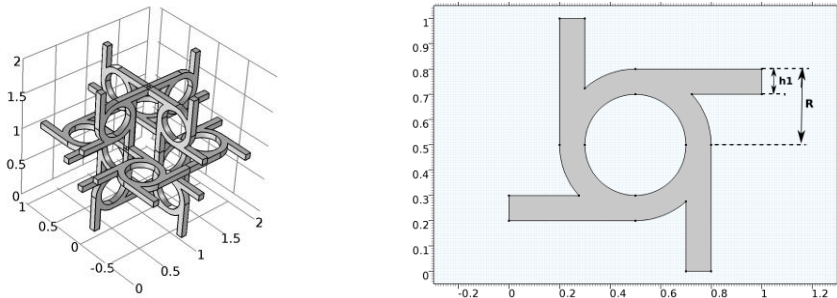
Linear constitutive equation - Hooke's law

$$\boldsymbol{\sigma} = \mathbf{D} \cdot \boldsymbol{\varepsilon}, \quad (3.3)$$

where  $\mathbf{D}$  is elasticity tensor and  $\boldsymbol{\sigma}$  is stress tensor,  $\boldsymbol{\varepsilon}$  is strain tensor.

## THREE-DIMENSIONAL ANTI-TETRA-CHIRAL STRUCTURE

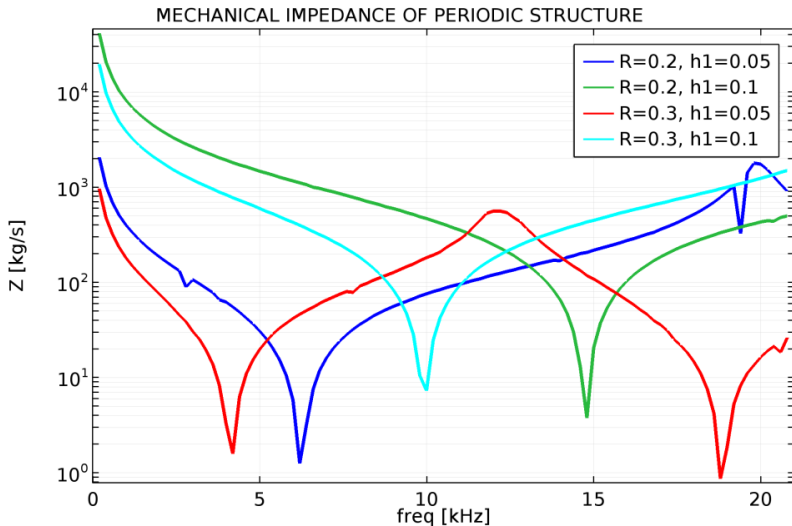
In this research three-dimensional anti-tetra-chiral structure is analyzed as a periodic structure with the unit cell (UC) presented at Figure 1. Influence of geometric parameters of a UC of the periodic structure on dynamic properties of the structure is investigated.

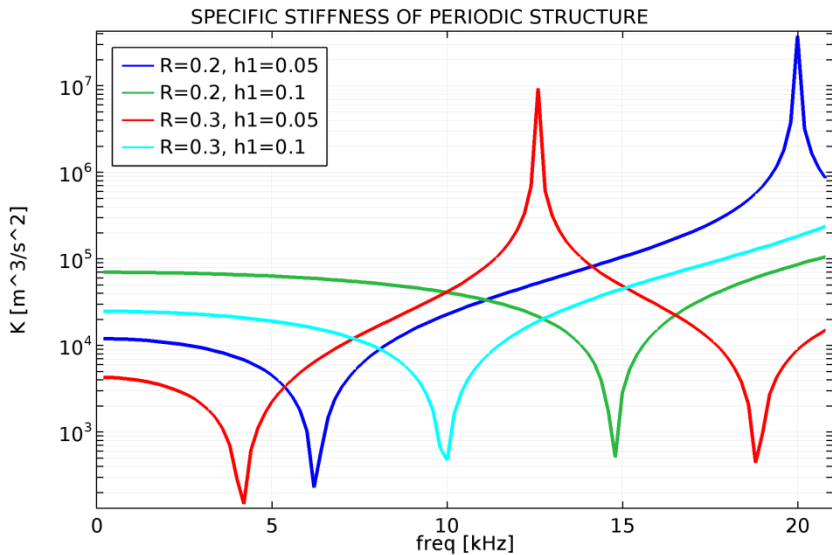


**Figure:** Unit cell of the three-dimensional anti-tetra-chiral periodic auxetic structure.

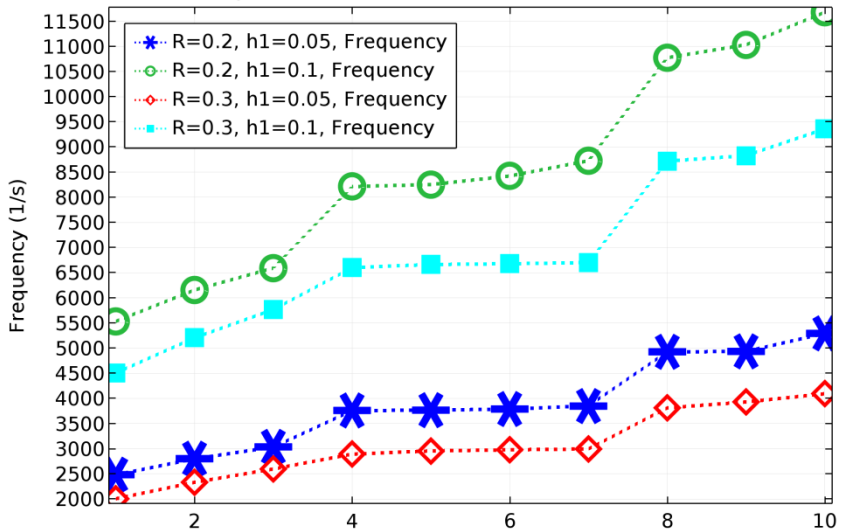
# EXAMPLE 1. MECHANICAL IMPEDANCE, UNIT CELL - 2 CM BOX

Frequency range (0.2 , 20) kHz, step 200 Hz, 100 steps



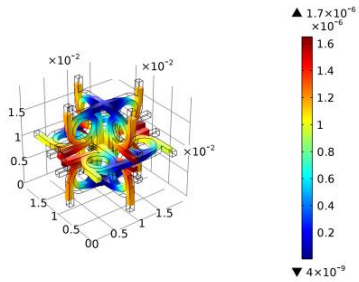


EIGENFREQUENCY OF UNIT CELL OF PERIODIC STRUCTURE

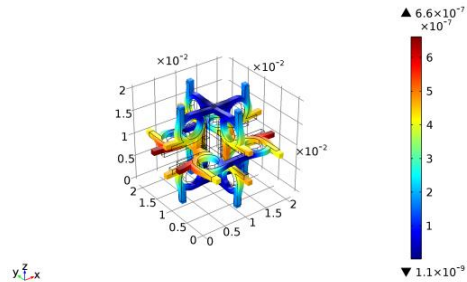


# DEFORMATION OF UC OF PERIODIC STRUCTURE

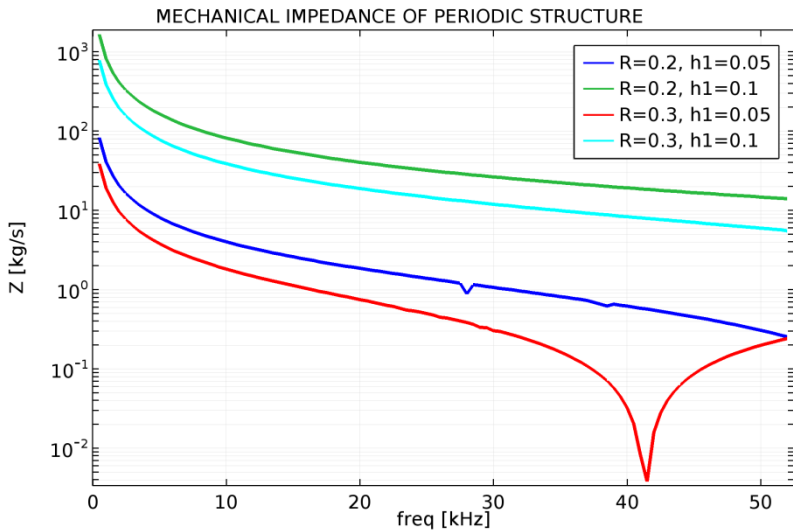
freq(1)=200 Surface: Total displacement (m)

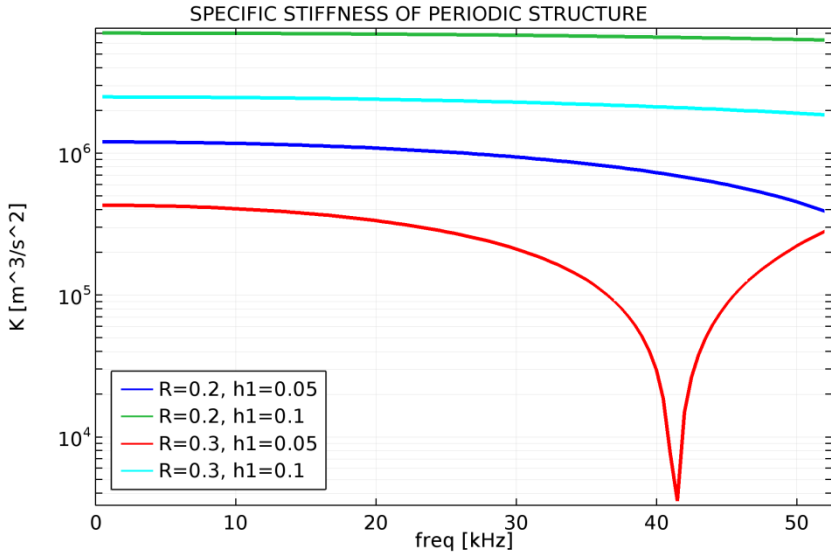


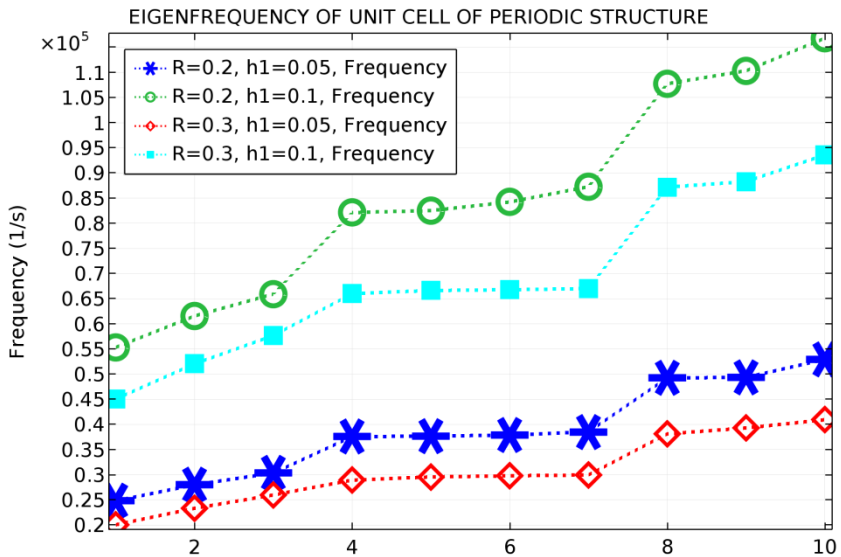
freq(100)=20000 Surface: Total displacement (m)



**EXAMPLE 2. MECHANICAL IMPEDANCE, UNIT CELL - 1 mm BOX**  
**Frequency range (0.5 , 50) kHz, step 500 Hz, 100 steps**

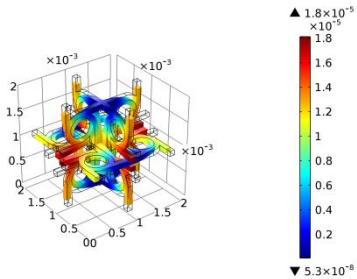






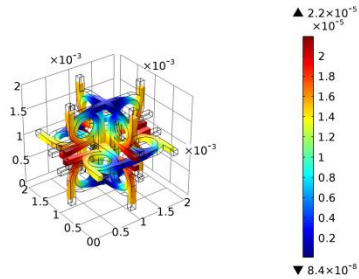
# DEFORMATION OF UC OF PERIODIC STRUCTURE

freq(60)=30000 Surface: Total displacement (m)



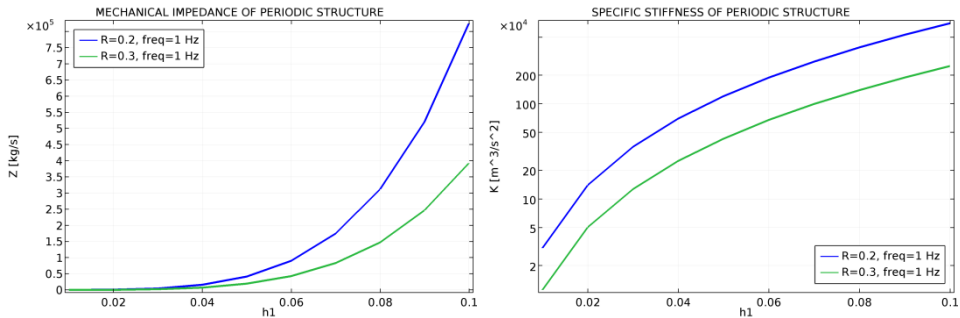
y z  
x

freq(100)=50000 Surface: Total displacement (m)



y z  
x

# INFLUENCE OF SIZE OF RIBS SQUARE CROSS-SECTION



# THANK YOU FOR YOUR ATTENTION

## ***ACKNOWLEDGMENTS***

*This work has been supported by a grant from the Ministry of Science and Higher Education in Poland: 02/21/DSPB/3513/2018. The simulations have been made at the Institute of Applied Mechanics, Poznan University of Technology.*

## REFERENCES

1. **A.E.H. Love**, A Treatise on the Mathematical Theory of Elasticity, Cambridge University Press, Cambridge 1892.
2. **W. Voigt**, Lehrbuch der Kristallphysik, B. G. Teubner-Verlag, Leipzig Berlin, 1928.
3. L.J. Gibson, The elastic and plastic behaviour of cellular materials, University of Cambridge, Churchill College (doctoral thesis) **1981**.
4. L.J. Gibson, M.F. Ashby, G.S. Schayer, C.I. Robertson, The mechanics of two-dimensional cellular materials. Proc. Roy. Soc. Lond. A **1982**, **382**, 25–42.
5. L. J. Gibson and M. F. Ashby, The Mechanics of Three-Dimensional Cellular Materials, Proc. R. Soc. Lond. A **1982** 382, 43-59. DOI: 10.1098/rspa.1982.0088
6. **G.N. Greaves, A.L. Greer, R.S. Lakes, T. Rouxel**, Poisson's ratio and modern materials, Nature Materials 10(11), pp. 823–37 (2011).
7. **Y. Prawoto**, Seeing auxetic materials from the mechanics point of view: A structural review on the negative Poisson's ratio, Computational Materials Science, 58, pp. 140–153 (2012).
8. **J.C.A Elipe, A.D. Lantada**, Comparative study of auxetic geometries by means of computer-aided design and engineering, Smart Mater. Struct., 21(10), 105004 (2012).
9. **T.C. Lim**, Auxetic Materials and Structures, Springer, Singapore 2015.
10. **K.K. Saxena, R. Das, E.P. Calius**, Three decades of auxetics research—Materials with negative Poisson's ratio: A review, Adv. Eng. Mater. 18, 1847-1870 (2016).
11. **H.M.A. Kolken, A.A. Zadpoor**, Auxetic mechanical metamaterials, RSC Adv., 7, 5111 (2017).
12. **X. Ren, R. Das, P. Tran, T. Duc Ngo, and Yi Min Xie**, Auxetic metamaterials and structures: A review, Smart Mater. Struct. **27**, 2 (2018).
13. **O. Duncan, T. Shepherd, C. Moroney, L. Foster, P.D. Venkatraman, K. Winwood, T. Allen, A. Alderson**, Review of Auxetic Materials for Sports Applications: Expanding Options in Comfort and Protection. Appl. Sci. 2018, 8, 941 (2018).

14. **R. Plunkett (editor)**, Colloquium on Mechanical Impedance Methods for Mechanical Vibrations, Noise Control vol. 5, no. 32 (1959). (doi:10.1121/1.2369363)
15. **P.L. Gatti, V. Ferrari**, Applied Structural and Mechanical Vibrations, CRC Press Taylor & Francis Group, New York, 2014.
16. **Frank J. On**, Mechanical Impedance Analysis For Lumped Parameter Multi-Degree Of Freedom / Multi-Dimensional Systems, National Aeronautics And Space Administration Washington, D. C., **1967**.

## REFERENCES

1. R.F. Almgren, An isotropic three-dimensional structure with Poisson's ratio  $=-1$ , Journal of Elasticity 15, pp.427-430 (1985).
2. K.W. Wojciechowski, Constant thermodynamic tension Monte Carlo studies of elastic properties of a two-dimensional system of hard cyclic hexamers, Molecular Physics 61, 1247-1258 (1987).
3. R.S. Lakes, Foam structures with a negative Poisson's ratio, Science 235, 1038-1040 (1987).
4. T.C. Lim, Auxetic Materials and Structures, Springer-Verlag, Singapur, 2015.
5. J.C. Álvarez Elipe, A. Díaz Lantada, Comparative study of auxetic geometries by means of computer-aided design and engineering, Smart Materials and Structures 21(10), 105004 (2012).
6. **M. Ruzzene, Vibration and sound radiation of sandwich beams with honeycomb truss core, Journal of Sound and Vibration 277, 741-763 (2004).**
7. **A. Spadoni, M. Ruzzene, F. Scarpa, Dynamic response of chiral truss-core assemblies, Journal of Intelligent Material Systems and Structures 17 (11), 941-952 (2006).**
8. **A. Spadoni, M. Ruzzene, Structural and acoustic behavior of chiral truss-core beams, Journal of Vibration and Acoustics, 128(5), 616-26 (2006).**
9. **R.R. Galgalikar, Design automation and optimization of honeycomb structures for maximum sound transmission loss, Clemson University, 2012.**

10. **H. Joshi, Finite Element Analysis of effective mechanical properties, vibration and acoustic performance of auxetic chiral core sandwich structures, All Theses. Paper 1723, Clemson University, Clemson, South Carolina, 2013.**
11. **B. Howell, P. Prendergast, L. Hansen, Examination of acoustic behavior of negative Poisson's ratio materials, *App. Acoust.* 43, 141–148 (1994).**
12. **I. Chekkal, M. Bianchi, C. Remillat, F.-X. Bécot, L. Jaouen, F. Scarpa, Vibro-Acoustic Properties of Auxetic Open Cell Foam: Model and Experimental Results, *Acta Acustica United with Acustica Vol.* 96, 266 – 274 (2010).**
13. **Harijono Djojodihardjo, Vibro-acoustic analysis of the acoustic-structure interaction of flexible structure due to acoustic excitation, *Acta Astronautica*, <http://dx.doi.org/10.1016/j.actaastro.2014.11.026>**
14. T. Strek, H. Jopek, M. Nienartowicz, Dynamic response of sandwich panels with auxetic cores, *Phys. Status Solidi B* 252(7), 1540–1550 (2015).
15. E. Idczak, T. Strek, Transmission Loss of Auxetic Lattices Vibration, *Applied Mechanics and Materials* 797, 282-289 (2015).
16. A.W. Lipsett, A.I. Beltzer, Reexamination of dynamic problems of elasticity for negative Poisson's ratio, *J. Acoust. Soc. Am.* 84, 2179–2186 (1988).
17. A. Spadoni, M. Ruzzene, F. Scarpa, Dynamic response of chiral truss-core assemblies, *J. Int. Mat. Syst. Struct.* 17, 941–952 (2006).
18. F. Scarpa, P.G. Malischewsky, Some new considerations concerning the Rayleigh-wave velocity in auxetic materials, *Physica Stat. Solidi B* 245, 578–583 (2008).
19. A. London, Methods for determining sound transmission loss in the field, Research Paper RP1388, Part of Journal of Research of the National Bureau of Standards, Volume 26 (1941).
20. T.D. Rossing, Handbook of Acoustic, Springer, LLC New York, 2007.
21. T. Strek, Finite Element Modelling of Sound Transmission Loss in Reflective Pipe, Finite Element Analysis, David Moratal (Ed.), 663-684, Sciyo, 2010.

## TRANSMISSION LOSS

The difference between the sound energy on one side of the system and that radiated from the second side (both expressed in decibels) is called the transmission loss.

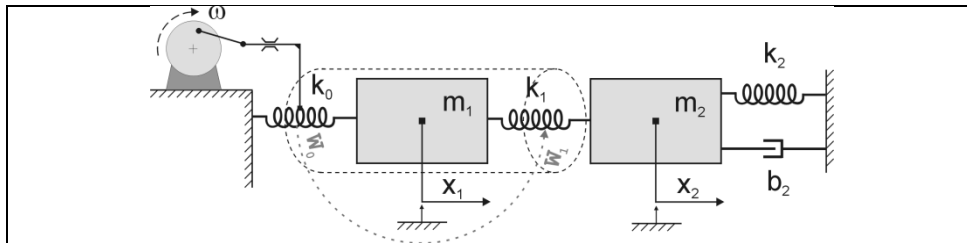
Transmission loss (TL) is given by

$$TL = 10 \log \frac{W_{in}}{W_{out}}, \quad (1.1)$$

where  $W_{in}$  denotes the incoming power at the inlet,  
 $W_{out}$  denotes the transmitted (outgoing) power at the outlet.

## MODEL OF MECHANICAL SYSTEM

Masses (2), springs (3) and damper.



Powers:  $W_0$ ,  $W_1$  - of spring with the spring constant  $k_0$  and  $k_1$ , respectively ,

$$W_0(t) = \frac{1}{2} k_0 \cdot x_{10}^2$$

$$W_1(t) = \frac{1}{2} k_1 \cdot (x_{20} - x_{10})^2$$

(1.2)

where:  $x_{10}$ ,  $x_{20}$  are amplitudes of harmonic motion of masses.

## EQUATIONS OF MASSES MOTION

Assuming that engine generates extortion force applied to system through spring, we get following equations of masses motion

$$m_1 \frac{\partial^2 x_1}{\partial t^2} + k_1(x_1 - x_2) = k_0 x_1, \quad (1.3)$$

$$m_2 \frac{\partial^2 x_2}{\partial t^2} + k_1(x_2 - x_1) + k_2 x_2 + b_2 \frac{\partial x_2}{\partial t} = 0. \quad (1.4)$$

Let us assume a time-harmonic motion of masses

$$x_1(t) = x_{10} e^{i\omega t} \quad x_2(t) = x_{20} e^{i\omega t}. \quad (1.5)$$

Substituting (1.5) in eq. (1.4) we get

$$-m_2 \omega^2 x_{20} + k_1(x_{20} - x_{10}) + k_2 x_{20} + b_2 i \omega x_{20} = 0, \quad (1.6)$$

and finally

$$x_{20} = \frac{-k_1 P_0}{k_1^2 - (k_1 - m_1 \omega^2)(k_1 + k_2 + i b_2 \omega - m_2 \omega^2)}. \quad (1.7)$$

Transmission loss of mechanical power  $TL$  in vibrating system is

$$TL = 10 \log \left| \frac{W_0}{W_1} \right| = 10 \log \left| \frac{k_0 x_{10}^2}{k_1 (x_{20} - x_{10})^2} \right| = 10 \log \left| \frac{k_0}{k_1} \right| + 20 \log \left| \frac{x_{10}}{x_{20} - x_{10}} \right| \quad (1.8)$$

where

$$\frac{x_{10}}{x_{20} - x_{10}} = - \frac{\frac{k_1}{k_2} + 1 + i \frac{b_2}{k_2} \omega - \frac{m_2}{k_2} \omega^2}{1 + i \frac{b_2}{k_2} \omega - \frac{m_2}{k_2} \omega^2}, \quad (1.9)$$

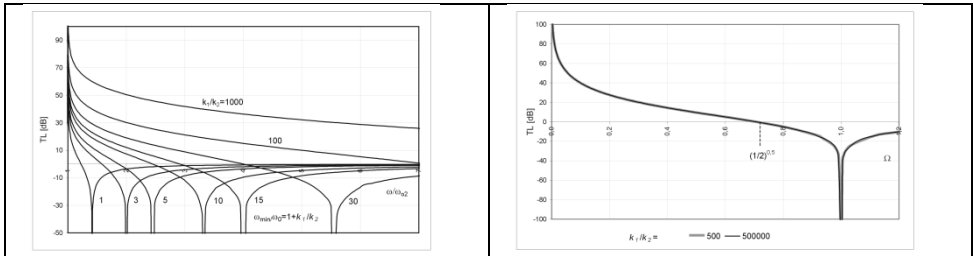
Assuming  $k_0 = k_1$ ,  $b_2 = 0$  and substituting (1.9) in (1.8), transmission loss of mechanical power in vibrating system without damping is

$$TL = 20 \log \left| \frac{x_{01}}{x_{02} - x_{01}} \right| = 20 \log \left| \frac{k_1/k_2}{(\omega/\omega_{02})^2 - 1} - 1 \right| = 20 \log \left( \frac{1}{\Omega^2} - 1 \right), \quad (1.10)$$

where:  $\omega_{02} = \sqrt{k_2/m_2}$  is called the undamped angular frequency of the receiver

environment;  $\Omega = \sqrt{\frac{(\omega/\omega_{02})^2 - 1}{k_1/k_2}}$  for  $\omega > \omega_{02}$  is reduced angular frequency of vibrating system.

## TRANSMISSION LOSS OF MECHANICAL SYSTEM (with $b_2=0$ )



## TRANSMISSION LOSS OF MECHANICAL SYSTEM (with $b_2>0$ )

